

Displacement damage in Hydrogenated Amorphous Silicon p-i-n diodes and charge selective contacts detectors.

M. Menichelli¹, M. Bizzarri^{1,2}, M. Boscardin^{3,4}, L. Calcagnile⁵, M. Caprai¹, A.P. Caricato⁵, G.A.P. Cirrone⁶, M. Crivellari⁴, I. Cupparo⁷, G. Cuttone⁶, S. Dunand⁸, L. Fanò^{1,2}, B. Gianfelici^{1,2}, O. Hammad⁴, M. Ionica¹, K. Kanxheri¹, M. Large¹⁰, G. Maruccio⁵, A.G. Monteduro⁵, F. Moscatelli^{1,9}, A. Morozzi¹, A. Papi¹, D. Passeri^{1,11} *Senior Member IEEE*, M. Pedio^{1,9}, M. Petasecca¹⁰ *Member, IEEE*, G. Petringa⁶, F. Peverini^{1,2}, G. Quarta⁵, S. Rizzato⁵, A. Rossi^{1,2}, G. Rossi¹, A. Scorzoni^{1,11}, L. Servoli¹, C. Talamonti⁷, G. Verzellesi^{3,12}, N. Wyrsh⁸.

Abstract— Hydrogenated amorphous silicon is a well known detector material for its radiation resistance. This study concerns 10 μm thickness, p-i-n and charge selective contacts planar diode detectors which were irradiated with neutrons at two fluence values: 10^{16} $n_{\text{eq}}/\text{cm}^2$ and 5×10^{16} $n_{\text{eq}}/\text{cm}^2$. In order to evaluate their radiation resistance, detector leakage current and response to X-ray photons have been measured. The effect of annealing for performance recovery at 100°C for 12 and 24 hours has also been studied. The results for the 10^{16} $n_{\text{eq}}/\text{cm}^2$ irradiation show a factor 2 increase in leakage current that is completely recovered after annealing for p-i-n devices while charge selective contacts devices show an overall decrease of the leakage current at the end of the annealing process compared to the measurement before the irradiation. X-ray dosimetric sensitivity degrades, for this fluence, at the end of irradiation but partially recovers for charge selective contacts devices and increases for p-i-n devices at the end of the annealing process. Concerning the 5×10^{16} $n_{\text{eq}}/\text{cm}^2$ irradiation test (for p-i-n structures only), due to the activation that occurred during the irradiation phase, the results were taken after 146 days of storage at around 0° C, during this period, a self-annealing effect may have occurred. Therefore the results after annealing show a small but noticeable degradation in leakage current and x-ray sensitivity, after irradiation and storage.

I. INTRODUCTION

RADIATION damage effects in Hydrogenated Amorphous Silicon (a-Si:H) have been extensively studied in the field of solar panels for Space applications [1,2,3]. Concerning the radiation resistance for the usage of this material in particle flux measurement, a fundamental reference paper is ref. [4], where a 32 μm thick n-i-p diode has been used for a proton beam monitoring experiment at high fluencies (up to about 10^{16} p/cm²). The resulting increment in the leakage current of the diode after 7×10^{15} p/cm² was measured to be only a factor of 2 (crystalline silicon detectors, after more than 20 years of technological R & D, have an increment of leakage current by a factor 50-100 for similar fluencies) and this degradation was completely reversed after 24 hours of annealing in air at 100 °C. Recovery was also obtained for charge collection efficiency after irradiation and subsequent annealing.

Although a-Si:H has such a remarkable radiation resistance, a planar detector fabricated using this material possesses a primary limitation in a poor signal-to-noise ratio for the detection of MIP (Minimum Ionizing Particle) that has yet to exceed the value of 5. The reason for this is the very high voltage needed to deplete a detector (in the order of 10 V/ μm) that generates a very high leakage current that can reach the order of 1 $\mu\text{A}/\text{cm}^2$; moreover, the charge collection efficiency is below 50% for a 30 μm thick diode.

A possible solution for these problems is a 3D detector geometry that allows to keep a relatively small inter-electrode distance (in the order of 25-30 μm) with detector thickness around 100 μm in order to increase the total charge generated in the detector by a MIP. The reduction of the distance between the electrodes is a crucial factor for keeping the leakage current low reducing the noise [5,6,7].

One of the main technological challenges in the fabrication of these devices is the doping on the finger type (or trench type) electrodes of the device. The doping techniques to be used in order to solve this problem, should provide an uniform coating of the surfaces of the etched cylindrical holes (or trenches). We have found two possible techniques that can fulfill this goal: a) atomic layer deposition of charge selective oxides: MoO_x for hole selective contacts and TiO₂ or

This work was partially supported by the “Fondazione Cassa di Risparmio di Perugia” RISAI project n. 2019.0245.

¹ INFN, Sez. di Perugia, via Pascoli s.n.c. 06123 Perugia (ITALY)

² Dip. di Fisica e Geologia dell’Università degli Studi di Perugia, via Pascoli s.n.c. 06123 Perugia (ITALY)

³ INFN, TIPFA Via Sommarive 14, 38123 Povo (TN) (ITALY)

⁴ Fondazione Bruno Kessler, Via Sommarive 18, 38123 Povo (TN) (ITALY)

⁵ INFN and Dipartimento di Matematica e Fisica “Ennio de Giorgi” dell’Università di Lecce, Via per Arnesano, 73100 Lecce (ITALY)

⁶ INFN Laboratori Nazionali del Sud, Via S. Sofia 62, 95123 Catania (ITALY)

⁷ INFN and Dipartimento di Fisica e Astronomia dell’Università di Firenze, Via Sansone 1, 50019 Sesto Fiorentino (FI) (ITALY)

⁸ Ecole Polytechnique Fédérale de Lausanne (EPFL), Institute of Electrical and Microengineering (IME), Rue de la Maladière 71b, 2000 Neuchâtel, (SWITZERLAND).

Aluminum doped ZnO (AZO) for electron selective contacts and b) Ion implantation of Phosphorous (n-type) or Boron (p-type).

In this paper, displacement damage radiation testing data using neutrons will be shown, the total displacement dose obtained with neutrons is larger, but comparable, in the NIEL approximation, to the displacement dose of ref.[4] that was obtained with protons. Moreover, the annealing procedure carried out on this work is the same adopted in ref. [4]. The main differences between the two measurements are a) the thickness of the diode (10 μm for this study 32 μm in ref. [4]), b) the type of damage: purely displacement damage here and a combination of total ionizing dose and displacement damage in ref. [4], c) the flux sensitivity measurement: flux measurements of protons in ref. [4] and x-ray flux measurements for this paper. The present work shows a neutron radiation test with doses above $10^{16} n_{\text{eq}(1\text{MeV})}/\text{cm}^2$ of a-Si:H detectors where the dominant mechanism is displacement damage, subsequent proton radiation damage tests and total ionizing dose tests with x-rays will be performed in the next future and the results will be published in forthcoming papers. The data here presented were collected during a radiation test performed in the framework of the INFN 3D-SiAm project which has the goal to fabricate and test a-Si:H 3D detectors and also of the INFN HASPIDE experiment which has the goal of fabricating radiation flux measurement devices for beam monitoring, particle fluxes measurements in solar events and neutron flux measurements; these devices will be fabricated on flexible substrates. The tests described here have been performed using planar prototype p-i-n and charge selective contact detectors developed for these experiments.

II. THE TESTED DEVICES AND THE TEST PROCEDURE

Three different device types have been irradiated during this irradiation session: a) Vertical p-i-n diode devices in square pads. b) Vertical p-i-n diode devices in strips c) Vertical charge selective contacts diodes in square pads.

Configuration (a) is shown in Fig. 1a, it is a 3 x 2 diode array of p-i-n vertical diodes where a 10 μm layer of a-Si:H is deposited on a p-type crystalline Silicon low resistivity substrate (thickness 300 μm); on the top of this layer the 6 n-i junctions having $0.5 \times 0.5 \text{ mm}^2$ dimensions are deposited via ion implantation (500 nm implantation depth) of phosphorous. Passivation with SiO_2 (160 nm deposited by PECVD) and diode metallization with chromium + aluminum (5nm Cr + 500 nm Al) is added on the top of the device. The device is then packaged in a ceramic DIL Package (P/N: CSB02219).

Configuration (b) (shown in Fig.1b) is an 8-strip device fabricated using the same process described for configuration (a), where the strips have dimensions $5 \times 0.2 \text{ mm}^2$.

Configuration (c) (Fig. 1c) has 4 planar charge selective contact devices each having $4 \times 4 \text{ mm}^2$ surface on a 8.2 μm thick a-Si:H substrate; molybdenum oxide is adopted for hole selective contacts is placed on top of the device, while the bottom electron selective contact is aluminum-zinc doped oxide (AZO). These detectors have been described in Ref. [8].

The tests were performed according to the following procedure:

1. Pre-irradiation leakage current versus bias voltage measurements test and measured current versus dose rate for exposure to an x-ray tube biased at 30 kV at different tube currents. X-ray dose-rate versus tube current calibration procedure is described below.
2. Irradiation with neutrons of two separate detectors sets; each set has been irradiated at different fluencies (see below)
3. Post irradiation measurements are basically a repetition of the test described at point 1 after irradiation.
4. Annealing on air (phase-1) of irradiated sample in an oven at 100 $^\circ\text{C}$ for 12 hours.
5. Post phase-1 annealing measurements with the procedure described at point 1
6. Annealing in air (phase-2) of irradiated sample in an oven at 100 $^\circ\text{C}$ for additional 12 hours.
7. Post phase-2 annealing measurements with the procedure described at point 1.

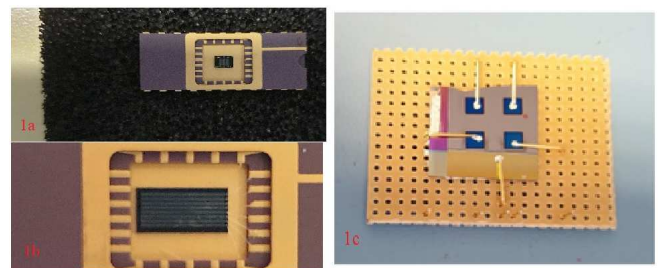


Fig. 1. Detector configurations tested for displacement damage a) Configuration (a) 2 x 3 pad detector array with n junction implanted and is packaged on a ceramic package b) configuration (b) 8 strip detector with n junction implanted. c) Configuration (c) has 4 charge selective contact devices having $4 \times 4 \text{ mm}^2$ surface and 8.2 μm a-Si:H thickness.

The detectors have been irradiated with neutron at the Jozef Stefan Institute in Ljubljana (Slovenia) with two different fluencies of $1 \times 10^{16} n_{\text{eq}(1\text{MeV})}/\text{cm}^2$ and $5 \times 10^{16} n_{\text{eq}(1\text{MeV})}/\text{cm}^2$, in two different batches.

The neutron spectrum used in this irradiation test is reported in Fig.2, the total fluence in units of $n_{\text{eq}(1\text{MeV})}/\text{cm}^2$ is determined by integral of the convolution of this spectrum with the dose damage versus kinetic energy curve of neutrons; in order to obtain the number of 1 MeV neutron equivalent the

⁹ CNR-IOM, via Pascoli s.n.c. 06123 Perugia (ITALY)

¹⁰ Centre for Medical Radiation Physics, University of Wollongong, Northfields Ave Wollongong NSW 2522, (AUSTRALIA).

¹¹ Dip. di Ingegneria dell'Università degli studi di Perugia, via G.Duranti 06125 Perugia (ITALY)

¹² Dip. di Scienze e Metodi dell'Ingegneria, Università di Modena e Reggio Emilia, Via Amendola 2, 42122 Reggio Emilia (ITALY)

results of this integral it is divided by $2.037 \text{ keV cm}^2/\text{g}$ which is the displacement damage dose of one neutron having 1 MeV kinetic energy.

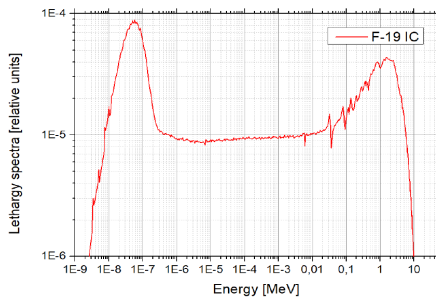


Fig.2 Spectrum of neutron used in this irradiation test [11].

As previously stated during the tests, we measured the leakage current at various bias voltages and the detector current under x-ray irradiation at different dose rates this quantity is related to the long term charge collection efficiency which is a useful quantity to determine the performance of devices when used in a beam monitoring application. From the linear fit of these data, we extracted the dosimetric sensitivity. The detectors were biased using a Keithley 2410-C and a Keithley 2400 SMU that measure currents with a 10 pA resolution. X-rays were generated by a tube from Newton Scientific having 50 kV maximum voltage and 200 μA maximum current [9], the doses were measured using a Cobia Flex dosimeter equipped with a RTI T20 dose probe [10].

The x-ray test setup in Perugia is shown in Fig.3 and a typical doses versus tube current calibration curve is shown in Fig. 4. This calibration aim is to determine the correspondence between the x-ray flux generated by the current in the tube and the effective dose rate in the sample measured employing the Cobia flex dosimeter probe placed in the same position of the irradiated detector device.

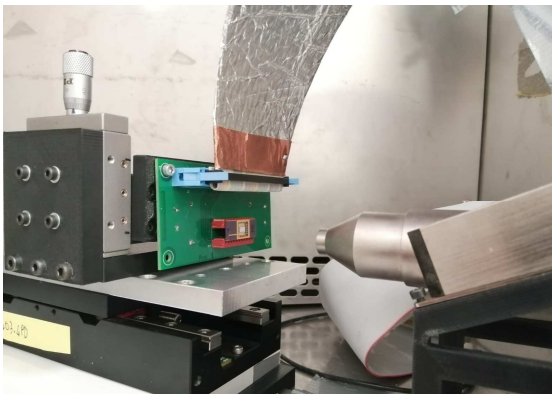


Fig. 3. Test setup for x-ray response measurement.

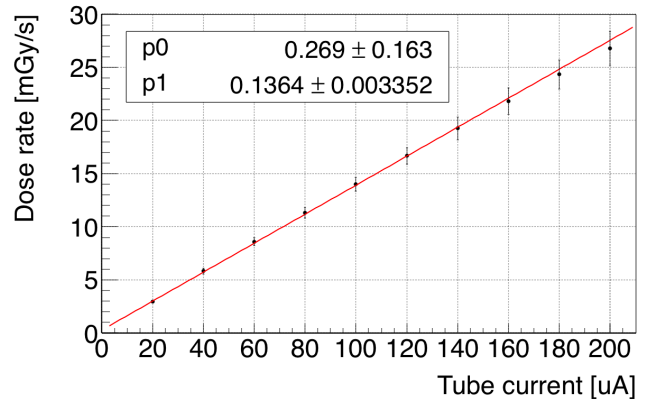


Fig.4 Typical calibration curve between dose and tube current at 30 kV tube voltage. The dose rate was measured by a Cobia Flex dosimeter with the probe placed in the same position of the DUT irradiated at various tube currents.

III. RESULTS AFTER $10^{16} \text{ NEQ}/\text{CM}^2$ IRRADIATION

We have tested one configuration (b) and one configuration (c) device after $10^{16} \text{ neq}/\text{cm}^2$ neutron irradiation.

The leakage current was measured for one p-i-n strip diode device and one charge selective contact device. In Fig.5 the leakage current on p-i-n is shown before and after irradiation and after 12 hours of annealing at 100°C as described in the previous chapter. Measurements were performed after 30 minutes of bias at the maximum voltage for device current stabilization.

Compared to pre-irradiation values an increment of leakage current can be observed after irradiation, especially at bias voltages below 70V. After 12 hours of annealing, a new measurement was performed and leakage current returned to pre-irradiation values at low bias voltage, becoming even lower at bias voltages higher than 50 V. This is in agreement with what was observed for protons in ref. [4].

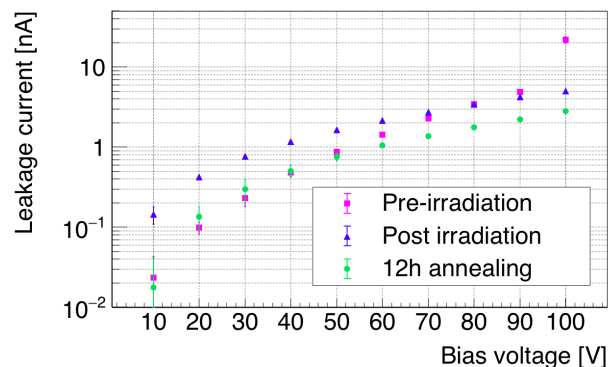


Fig.5 Leakage current versus bias voltage for p-i-n device. The measurement were taken before and after neutron irradiation and after 12 hours of annealing.

The leakage current of charge selective devices was also measured and it is shown in Fig.6. Also in this case we observe an increment of leakage current after the irradiation. The increment was higher at high values of the bias voltage and lower at low bias voltages. In this case, two annealing sessions were performed lasting 12 hours each at 100°C .

After the first 12 hours of annealing, the values of the

leakage current at various voltages were even lower than the pre-irradiation values. The additional 12 hours annealing session did not result in any further decrease in leakage current.

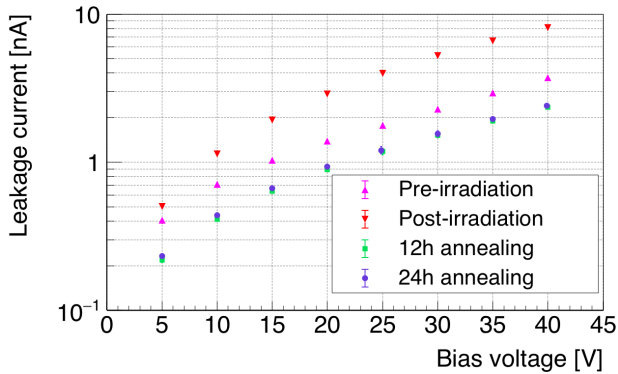


Fig.6 Leakage current versus bias voltage for charge selective contacts device. The measurement were taken before and after neutron irradiation and after 12 and 24 hours of annealing.

Radiation sensitivity and flux response to x-ray irradiation have been measured for these detectors in order to study the response to x-rays and to demonstrate their capability to measure radiation fluxes under severe radiation environments. For this purpose, we used the setup shown in fig.2 with the tube biased at 30 kV and dose rates from 0 to 24 mGy/s.

P-i-n diode device biased at 60 V gave the response shown in fig.7. The response was linear under all conditions and the sensitivity changed from 2.39 nC/cGy for the non-irradiated component to 1.13 nC/cGy after irradiation; after the 12 hours of annealing the sensitivity increased up to 3.0 nC/cGy. This increment is somehow comparable with the leakage current behavior where the leakage current increases after irradiation and decreases below the pre-irradiation value after annealing. It is important to mention that the points of the graph in fig. 7 are obtained by measuring the current under x-ray irradiation after subtracting the values of the leakage current. Errors in dose rate are evaluated from the uncertainty of the exact distance between the tube and the detector and for the current we took the standard deviation of measured values.

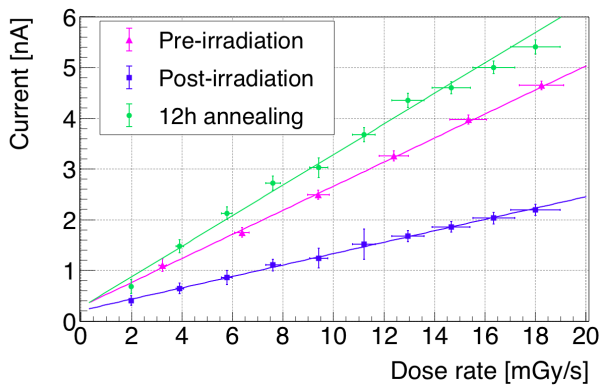


Fig. 7 P-i-n diode device response to x-ray irradiation versus dose rate. The measurement were taken before and after neutron irradiation and after 12 hours of annealing at 100°C.

Charge selective devices response to x-ray irradiation at various rates has been measured both at 0 V (photovoltaic mode typical of medical dosimeters) bias and 30 V bias (more suitable for beam monitoring); the results are shown in Fig. 8 and 9.

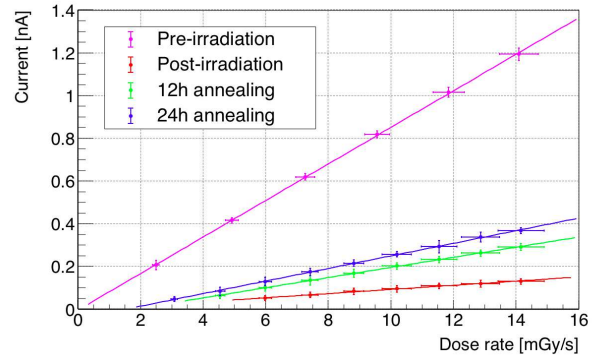


Fig.8 Charge selective contacts device (at 0V bias) response to x-ray irradiation versus dose rate. The measurement were taken before and after neutron irradiation and after 12 and 24 hours of annealing at 100°C

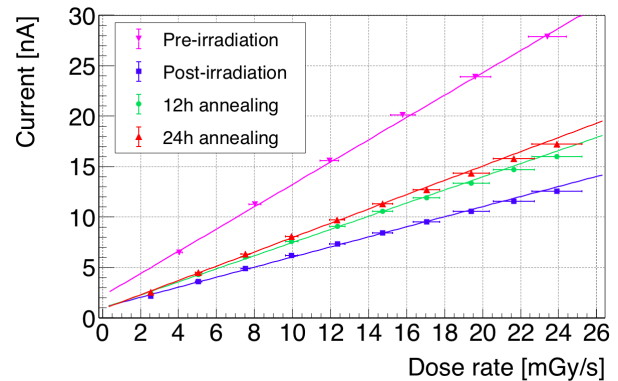


Fig.9 Charge selective contacts device (at 30V bias) response to x-ray irradiation versus dose rate. The measurement were taken before and after neutron irradiation and after 12 and 24 hours of annealing at 100°C.

It is worth noting that, from these data the recovery after irradiation is less evident than in the p-i-n diode device. The response is linear, especially when bias is applied; however, at 0 V the charge sensitivity is 0.86 nC/cGy for the non-irradiated component while after irradiation decreases by a factor of 8.6 (0.10 nC/cGy). The device partially recovers after 12 hours of annealing up to 0.24 nC/cGy and to 0.30 after 24 hours of annealing. The results obtained with a 30 V bias confirm this trend: the sensitivity before irradiation was 11.1 nC/cGy reduced by more than a factor 2 after neutron irradiation down to 5.0 nC/cGy, it partially recovers after 12 h annealing up to 6.5 nC/cGy and after 24h up to 7.2 nC/cGy. A summary table of these results is shown in Table I.

TABLE I
SENSITIVITY UNDER VARIOUS CONDITIONS FOR P-I-N DIODE AND CHARGE
SELECTIVE CONTACTS DEVICES AFTER 10^{16} N_{eq}/CM^2 NEUTRON IRRADIATION

Detector type and bias	Pre-rad Sensitivity (nC/cGy)	Sensitivity after irradiation (nC/cGy)	Sensitivity after 12h annealing (nC/cGy)	Sensitivity after 24h annealing (nC/cGy)
CSC at 30V bias	11.1 ± 0.3	5.0 ± 0.1	6.5 ± 0.2	7.2 ± 0.2
CSC at 0V bias	0.86 ± 0.03	0.10 ± 0.02	0.24 ± 0.02	0.30 ± 0.02
P-i-n diode at 60V	2.39 ± 0.09	1.13 ± 0.08	3.0 ± 0.1	-

IV. RESULTS AFTER 5×10^{16} N_{eq}/CM^2 IRRADIATION

One configuration (a) and one configuration (b) p-i-n diode devices were irradiated with 5×10^{16} n_{eq}/cm^2 neutron fluence.

After the irradiation the components were heavily activated and measurements could be carried out only after 146 days after the irradiation. Although during this time the components were kept at approximately $0^\circ C$ some self-annealing in air has may be occurred. This effect can explain the reason why for this measurement the actual annealing at the $100^\circ C$ temperature had a reduced effect compared with the measurements described in the previous section. Due to residual radioactivity after irradiation the components could not be shipped, hence the x-ray response was measured after irradiation and annealing at the JSI laboratory with a different setup. The x-ray tube that was used in Lubljana had a tungsten cathode, voltage in the 5-160 kV range with current in the range 0.5-50 mA and maximum power of 3 kW. Preliminary dosimetric measurements on the JSI setup were performed with the same instrument we used for the measurement described in the previous section for dose rate consistency of the two setups. A picture of the JSI x-ray setup is shown in Fig.10.

The leakage current for one of the configuration (a) devices is shown in Fig. 11. There is a relevant increase (by a factor of 2.5 at 100 V) in leakage current after irradiation that does not change after annealing probably due to self-annealing under storage as already mentioned at the beginning of this section. The larger error bars on the pre-irradiation curve are due to the different (and noisier) setup used.

Concerning configuration (b) device (Fig.12) we notice a decrease in leakage current after irradiation (and self-annealing). After the 12 hours of annealing at $100^\circ C$ the leakage current increased above the non-irradiated values and did not change significantly after 12 additional hours of annealing.

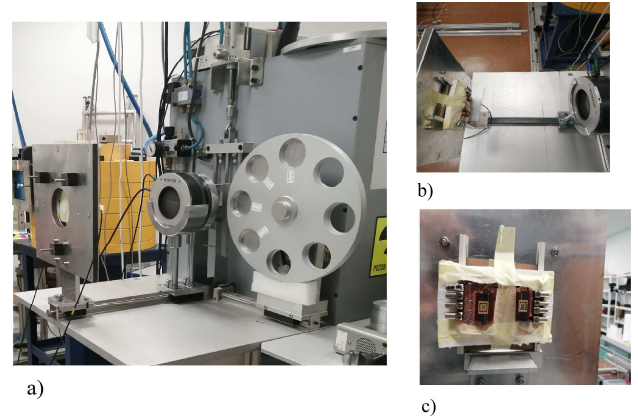


Fig.10 a) X-ray tube at JSI with monitoring ionization chamber and sample holder b) Top view of ionization chamber and sample holder c) samples on the holder irradiated simultaneously.

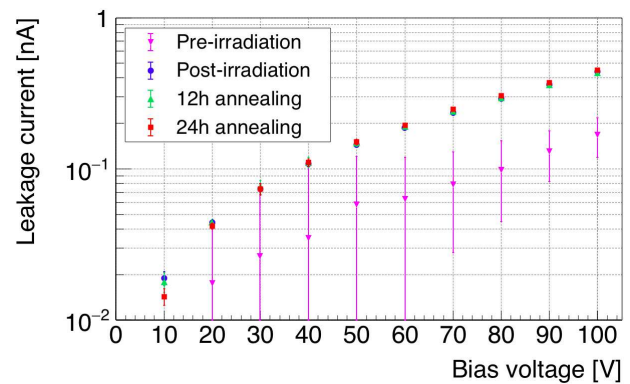


Fig. 11 Leakage current versus bias voltage for configuration (a) device. The measurements were taken before and after neutron irradiation and after 12 and 24 hours of annealing.

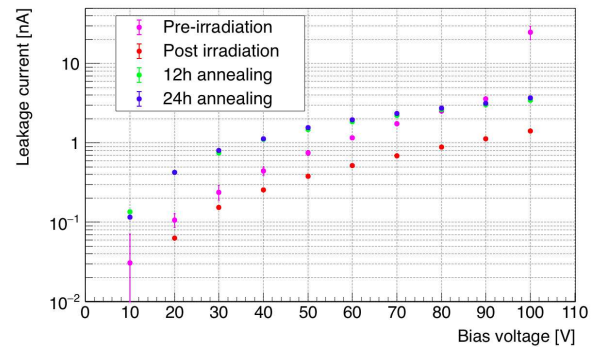


Fig. 12 Leakage current versus bias voltage for configuration (b) device. The measurements were taken before and after neutron irradiation and after 12 and 24 hours of annealing.

X-ray response was measured for both devices. Configuration (a) device (Fig.13) shows good linearity and a reduction of sensitivity from 1.94 to 0.57 nC/cGy after irradiation and auto-annealing. After 12 hours of annealing the sensitivity increased to 0.77 nC/cGy and after 24 hours of annealing increased additionally up to 0.84 nC/cGy.

Also, configuration (b) device shows very good linearity (Fig.14). After irradiation and auto-annealing the charge sensitivity was reduced from 2.55 to 0.74 nC/cGy. After 12 hours of annealing the sensitivity increased to 1.07 nC/cGy

and after 24 hours of annealing increased additionally up to 1.27 nC/cGy

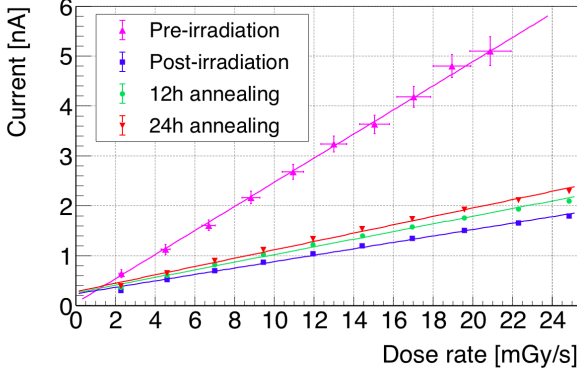


Fig. 13 Configuration (a) device response to x-ray irradiation versus dose rate. The measurement were taken before and after neutron irradiation and after 12 and 24 hours of annealing at 100°C.

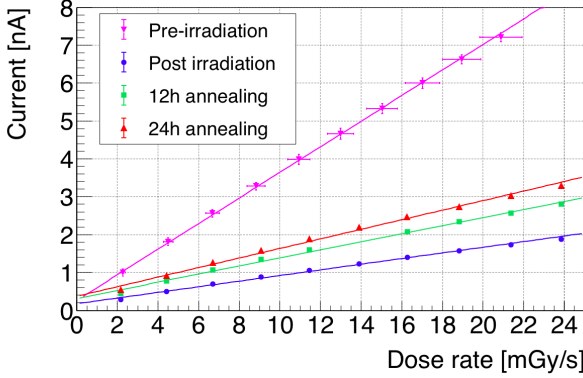


Fig. 14 Configuration (b) device response to x-ray irradiation versus dose rate. The measurement were taken before and after neutron irradiation and after 12 and 24 hours of annealing at 100°C.

A summary table of these measurements is shown in table II.

TABLE II
SENSITIVITY UNDER VARIOUS CONDITIONS FOR CONFIGURATION A AND B
DEVICES AFTER $5 \times 10^{16} \text{ n}_{\text{eq}}/\text{cm}^2$ NEUTRON IRRADIATION

Detector type and bias	Pre-rad Sensitivity (nC/cGy)	Sensitivity after irradiation (nC/cGy)	Sensitivity after 12h annealing (nC/cGy)	Sensitivity after 24h annealing (nC/cGy)
Configuration a device at 60V bias	1.94 ± 0.07	0.568 ± 0.005	0.769 ± 0.006	0.837 ± 0.006
Configuration b device at 60V bias	2.55 ± 0.08	0.737 ± 0.006	1.07 ± 0.01	1.27 ± 0.01

During sensitivity measurements, we also tested the stabilization of the time response of these devices. Figure 15 shows detector response with time before/during/after the application of x-ray (24 mGy/s dose rate) irradiation on a configuration (b) device before neutron irradiation and before and after the first 12 hours of annealing. From this figure we

can notice that the time response of the unirradiated sample is similar of the response after annealing (although reduced in amplitude) and the response before annealing seems to be faster than the response before irradiation although it shows a reduced amplitude as a consequence of a long-term charge efficiency reduction.

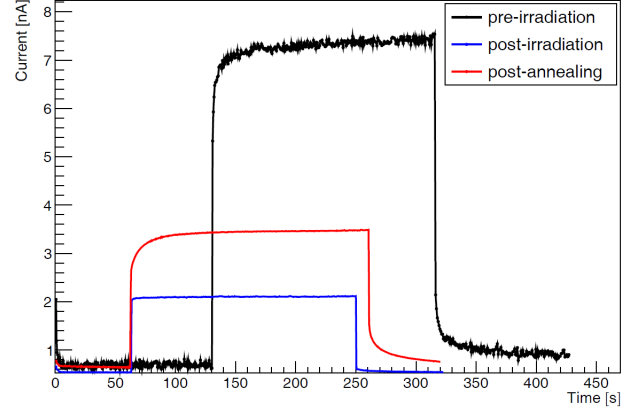


Fig. 15 Time response of the current before/during/after the x-ray irradiation test for a configuration (b) device tested with a dose rate of 24 mGy/s. The time response of the unirradiated sample is very similar of the response of the detector after the first 12 hours of annealing, while after irradiation the time response seems to be faster although the amplitude is reduced.

V. CONCLUSIONS

A total of four a-Si:H detector devices have been irradiated with neutron at the Jozef Stefan Institute reactor facility in Ljubljana (SLO). These detectors were designed in three different configurations:

- **Configuration a** Vertical p-i-n diode devices in square pads ($0.5 \text{ mm} \times 0.5 \text{ mm}$).
- **Configuration b** Vertical p-i-n diode devices in strips ($5 \text{ mm} \times 0.2 \text{ mm}$).
- **Configuration c** Vertical charge selective contacts diodes in square pads ($4 \text{ mm} \times 4 \text{ mm}$).

One device of configuration (b) and one configuration (c) were irradiated up to the total fluence of $1 \times 10^{16} \text{ n}_{\text{eq}}(1\text{MeV})/\text{cm}^2$ and then annealed for 12 hours (device type (b) and (c)) and 24 hours (device (c) only) at the temperature of 100 °C. After the irradiation, we observe an increment in leakage current more homogeneous at all bias voltages for configuration (c) device and more evident at low bias voltages for configuration (b) device. After 12 hours of annealing, the leakage current returned to the original value for the configuration (b) component and was reduced to about 50% for the configuration (c) device. The radiation sensitivity under non-zero bias was reduced by more than a factor 2 after irradiation and partially recovered (up to 65%) for the charge selective contact device and had a 25% increment compared to the original value for the configuration (b) device. From these data, we can infer that irradiation generates relevant damage in the two devices, and partial or total recovery is observed after annealing. Concerning the irradiation of one configuration (a) and one configuration (b) device up to fluencies $5 \times 10^{16} \text{ n}_{\text{eq}}/\text{cm}^2$ it is important to consider that due to activation the

two devices were measured only after 146 days from the end of neutron irradiation and these may have induced some auto-annealing making the successive 100 °C annealing less efficient in the recovery of the performances. Nevertheless the two devices, after 24 hours of annealing, recovered partially their performances. The radiation sensitivity, after the complete annealing process was 43% of the pre-rad value for configuration (a) and 50% for configuration (b). In the near future we plan to repeat the irradiation with protons in the few MeV range, combining the effect of displacement with the effect of the total ionizing dose. An investigation of the damage mechanism caused by neutron irradiation is above the scope of the present paper which is focussed to functional measurements in beam monitoring applications. A dedicated paper on this topic is under preparation and is based on soft X high resolution photoemission spectroscopy and atomic force microscopy [12]. Preliminarily, the main results of this work are that neutron irradiation causes the breaking of a high amount of Si-H bonds in the active material increasing the number of non-passivated bonds. This causes defects in the bandgap increasing the leakage current and decreasing charge collection efficiency (even in the long term) leading to the observed reduction in dosimetric sensitivity. It was also observed that the number of Si-H bonds tend to increase after annealing generating a partial recovery in terms of reduction of leakage current and increase of dosimetric sensitivity.

ACKNOWLEDGMENT

The authors wish to acknowledge the JSI personnel in particular Dr. Anze Jazbec and Dr. Matjaz Mihelic for their fundamental contribution during activation monitoring and x-ray tests. The p-i-n devices were developed by Fondazione Bruno Kessler (FBK) in the framework of FBK and INFN MiNaTAP agreement on a a-Si:H layer deposited by EPFL. Charge selective contacts devices were fully developed by EPFL. For this project, Matthew Large is sponsored by the AINSE Post Graduate Research Award (PGRA) – Australia.

REFERENCES

- [1] J.R. Srour et al. Damage Mechanism in Radiation-Tolerant Amorphous Silicon Solar Cells. *IEEE Trans. Nucl. Sci.* Vol. 45 pp. 2624-2631 1998
- [2] J. Kuendig et al. Thin film silicon solar cells for space applications: Study of proton irradiation and thermal annealing effects on the characteristics of solar cells and individual layers. *Solar Energy Materials & Solar Cells* Vol. 79 pp. 425–438, 2003.
- [3] H.C. Neitzert et al. “Investigation of the damage as induced by 1.7 MeV protons in an amorphous/crystalline silicon heterojunction solar cell”. *Solar Energy Materials & Solar Cells* Vol. 83 pp. 435–446 Jul 2004 doi: 10.1016/j.solmat.2004.01.035.
- [4] N. Wyrsh et al. “Radiation hardness of amorphous silicon particle sensors”. *J. Non-Cryst. Solids*, Vol. 352, pp. 1797–1800. Jun 2006. Doi: 10.1016/j.jnoncrysol.2005.10.035.
- [5] M.Menichelli et al. “Hydrogenated amorphous silicon detectors for particle detection, beam flux monitoring and dosimetry in high-dose radiation environment”. *JINST* Vol. 15, N.C04005 Apr. 2020. Doi: 10.1088/1748-0221/15/04/C04005

- [6] M.Menichelli et al. “3D Detectors on Hydrogenated Amorphous Silicon for particle tracking in high radiation environment”. *J. Phys.: Conf. Ser.* Vol. 1561 N.012016 Sept. 2020. doi:10.1088/1742-6596/1561/1/012016
- [7] M.Menichelli et al. “Fabrication of a Hydrogenated Amorphous Silicon Detector in 3-D Geometry and Preliminary Test on Planar Prototypes”. *Instruments*, Vol. 5, N. 32. Oct. 2021. Doi: /10.3390/instruments5040032
- [8] M.Menichelli et al. “Testing of planar hydrogenated amorphous silicon sensors with charge selective contacts for the construction of 3D detectors”. *JINST* 17 C03033 Mar. 2022. doi:10.1088/1748-0221/17/03/C03033
- [9] Datasheet available at <http://www.newtonscientific.com/50kv-10w-monoblock/> Last accessed 23rd June 2022
- [10] Specifications available at <https://rtigroup.com/products/cobia-rti-cobia-flex-r-f/#specification> Last accessed 23rd June. 2022
- [11] A. Jazbec private communication. 26th January 2021
- [12] F. Peverini, M. Pedio et al. “High Resolution Photoemission Study of neutron induced defects on hydrogenated amorphous silicon devices” paper in preparation to be submitted to *Nanomaterials*